BUTP-2002/03
LU TP 02-05
February 2002

Eta decays at and beyond $\mathbf{p^4}$ in Chiral Perturbation Theory[1]

Johan Bijnens[a] **and Jürg Gasser**[b]

[a]Department of Theoretical Physics, Lund University
Sölvegatan 14A, S-22362 Lund, Sweden

[b]Institute of Theoretical Physics, University of Bern
Sidlerstrasse 5, CH-3012 Bern, Switzerland

PACS: 12.39.Fe (Chiral Lagrangians), 13.40.Hq (Electromagnetic decays), 14.40.Aq (pi , K, and eta mesons), 12.15.Ff (Quark and lepton masses and mixing)

Abstract

An overview is given of Chiral Perturbation Theory and various applications to eta decays. In particular, the main decay $\eta \to 3\pi$ is discussed at the one-loop level, and estimates of the higher order corrections are given. The importance of p^6 and higher order effects in double Dalitz and $\eta \to \pi^0\gamma\gamma$ decays is pointed out. In all these cases the need for new experimental results is stressed.

[1]Talks presented at the Workshop on Eta Physics, Ångström laboratory, Uppsala, October 25-27, 2001; published in the proceedings (Physica Scripta Topical Issues T99 (2002) 34).

Contents

1 Introduction

Eta decays at high precision, both in measuring rare decays and in precisely determining kinematical distributions in the more common decays, have a high potential to teach us about various aspects of the strong interaction. In the view of the new experimental results to be expected from WASA at CELSIUS in Uppsala and KLOE at DAPHNE in Frascati and the ongoing work of the Crystal Ball, an overview of the present situation as regards some of the main eta decays is appropriate. The importance of these decays and measurements can be judged from the fact that they were the main focus of several theoretical talks presented at this workshop, in addition to the ones by the present authors there is also the contribution by Holstein[1] and by Ametller[2].

In this review we concentrate on chiral symmetry aspects for the main strong decay $\eta \to 3\pi$ and how it can be used to extract information on quark mass ratios. We will show how precise measurements of the slope parameters will lead to more refined theoretical predictions for the decay rate as a function of the quark mass ratio

$$\frac{m_s - \hat{m}}{m_d - m_u}\,. \tag{1}$$

A discussion of the decay $\eta \to 3\pi$ in Chiral Perturbation Theory (CHPT) and the use of dispersion theory to improve on the one-loop prediction is the main focus of this short review. In addition, a short overview is given of Dalitz ($\eta \to \gamma l^+ l^-$) and double Dalitz ($\eta \to l^+ l^- l'^+ l'^-$) decays, as well as of the process $\eta \to \pi^0\gamma\gamma$. We indicate why these are important quantities to be measured.

We first give a very short overview of chiral symmetry and its incorporation using effective field theory methods - known as Chiral Perturbation Theory - in Sect. 2. The decay $\eta \to 3\pi$ is then discussed at the purely perturbative level in CHPT at order p^4 in Sect. 3 and the estimates of higher orders using dispersion relations in Sect. 4. Section 5 is devoted to the Dalitz and double Dalitz decays, and the decay $\eta \to \pi^0\gamma\gamma$ is the subject of section 6. Our conclusions are presented in section 7.

2 Basics of CHPT

We cannot calculate all things we are interested in in the strong interaction directly from QCD. E.g. scattering amplitudes at low energies cannot be expressed as an expansion in the strong coupling constant because:

- At low energies the coupling constant becomes large.

- We deal with bound states which require always to go beyond a simple perturbation series.

So how can we calculate e.g. the cross-section of $\pi\pi$-scattering in QCD?

Two fundamental options are possible:

Lattice: This can be done using the methods developed by Lüscher[3] via QCD calculations at finite volume. The energy spectrum at finite volume depends on the $\pi\pi$ interaction. By measuring the lowest two-pion energy level, the $\pi\pi$ $S-$wave scattering lengths a_0^I can be obtained via

$$E^I = 2m_\pi - \frac{4\pi a_0^I}{m_\pi L^3} + \mathcal{O}(L^{-4}), \tag{2}$$

where I denotes isospin. There are first lattice results available which make use of this relation [4].

Effective Theory of QCD: Using the methods of *effective quantum field theory* (EFT) we can also evaluate cross-sections in QCD at low energies. We replace the QCD Lagrangian by the effective Lagrangian of Chiral Perturbation Theory (CHPT). We replace the quarks and gluons by the degrees of freedom which are relevant at low energies: π, K, η, p, n,.... This is the method most of this report is concerned with.

Chiral Perturbation Theory does reproduce for appropriately chosen coupling constants the S-matrix elements of QCD[5] and it allows to make very sharp predictions in some cases. As an example, we quote the recent result on the scattering length combination $a_0^0 - a_2^0$[6],

$$a_0^0 - a_0^2 = 0.265 \pm 0.004\,. \tag{3}$$

For earlier work at tree level and at one and two-loops accuracy, see [7, 8, 9].

We will now present the basics which underly the calculations of $\pi\pi \to \pi\pi$, $\eta \to \pi\pi\pi$, etc. in this approach.

2.1 Chiral Symmetry

Consider QCD with 3 flavours, u, d and s. Gluon interactions do not change the helicity of a quark, only mass terms couple the left and right handed helicity states. So in the limit where $m_u = m_d = m_s = 0$, the left-handed world cannot be turned into the right handed world. Now if all the masses are zero, there is also no way to distinguish the different flavours of quarks and we can continuously rotate one into the other. The QCD Lagrangian is thus invariant under

$$\begin{pmatrix} u \\ d \\ s \end{pmatrix}_H \longrightarrow V_H \begin{pmatrix} u \\ d \\ s \end{pmatrix}_H \quad ; \quad H = L, R\,, \tag{4}$$

separately for both helicities, left (L) and right (R). The matrices V_H are general unitary 3×3 matrices. So we have a global[2]

$$SU(3)_L \times SU(3)_R \tag{5}$$

chiral symmetry of QCD. This symmetry has 16 conserved currents and has thus 16 conserved charges. The vector charges $Q_V^i = Q_L^i + Q_R^i$ also annihilate the vacuum, but the axial charges $Q_A^i = -Q_L^i + Q_R^i$ produce a change on the vacuum:

$$Q_V^I|0\rangle = 0 \qquad Q_A^I|0\rangle \neq 0\,. \tag{6}$$

The symmetry of the QCD Lagrangian is *not* the symmetry of the vacuum. This is known as **spontaneous breakdown of chiral symmetry** or spontaneous chiral symmetry breaking ((S)χSB).

The 8 spontaneously broken axial symmetries require the existence of 8 Goldstone bosons which must be massless and pseudoscalar. They are the pions, kaons and eta. The Goldstone bosons also have zero interactions at zero energy. The expansion of CHPT is based on these facts.

Now, the fact that the quark masses are present and we can also have nonzero energies allows nonzero values for masses and interactions. E.g. the pion mass is an intricate mixture of the current quark mass, *explicit* χSB, and the quark vacuum expectation value, *spontaneous* χSB[14].

$$m_\pi^2 = -(m_u + m_d)\langle 0|\bar{u}u|0\rangle / F^2\,. \tag{7}$$

Similarly the pion scattering lengths do not vanish[7]

$$a_0^0 = \frac{7m_\pi^2}{32\pi F_\pi^2} = 0.159\,. \tag{8}$$

These predictions are not exact, they are the first term in a series expansion of momenta and the quark masses.

2.2 A systematic expansion

The amplitudes are expanded in powers of momenta and quark masses. The price paid for the generality is that order by order we get more terms,

$$\mathcal{L}_{\mathrm{CHPT}} = \mathcal{L}_2 + \mathcal{L}_4 + \mathcal{L}_6 + \dots\,, \tag{9}$$

where $\mathcal{L}_n$ contains terms with n-derivatives or equivalent. In amplitudes the derivatives turn into momenta such that the expansion converges at low momenta. As said earlier, quark masses are counted as two powers of momentum, this is

[2]The $U(1)$ parts of the groups play no role here, but see the contributions by Bass[10], Shore[11], Michael[12], Kroll and Feldmann[13] for their effects.

because Eq. (7) sets a quark mass to the pion mass squared. The structure of the Lagrangians $\mathcal{L}_n$ is fixed by chiral symmetry but the coupling constants are not.

In the strong and semileptonic mesonic sector, these Lagrangians are known and the parameters have conventional names:

$\mathcal{L}_2$: F_0, B_0 [15]

$\mathcal{L}_4$: $L_1, \ldots, L_{10}$ [16]

$\mathcal{L}_6$: $C_1, \ldots, C_{90}$ [17]

$\vdots$

These coupling constants (LEC's) are free in chiral perturbation theory, but are in principle calculable from QCD[3].

The Lagrangians $\mathcal{L}_{2,4,6,\ldots}$ allow to calculate S-matrix elements order by order in powers of momenta and quark masses. The main point is that order by order, only a limited number of terms can contribute, and the form of the contribution is completely fixed by chiral symmetry. So an amplitude can be expanded in powers

$$A = A_2 + A_4 + A_6 + \cdots , \tag{10}$$

with

A_2: tree graphs with vertices from $\mathcal{L}_2$. The form of the vertices is fixed by chiral symmetry.

A_4: tree graphs with vertices from $\mathcal{L}_2$ and one vertex from $\mathcal{L}_4$ or loop graphs with vertices from $\mathcal{L}_2$.

$\vdots$

This procedure is known as *Chiral Perturbation Theory* (CHPT).

In loop integrals one integrates over all momenta, from eV to the Planck mass and beyond, yet we always use the vertices from the effective Lagrangian constructed to reproduce the amplitude at low energies. This is not a contradiction, the high energy behaviour of the loop integrals is irrelevant in the sense that this is the part that is absorbed by the coupling constants. In this way, different regularizations can be used to cut-off the integrals and the difference in different ways of doing it is absorbed by using different values of the coupling constants. The final result is always independent of the regularization used. In practice we nearly always use dimensional regularization since it preserves chiral symmetry throughout the calculation reducing the need for technically complicated subtractions to restore symmetries.

[3] For some attempts to determine them from lattice QCD, see Ref. [18].

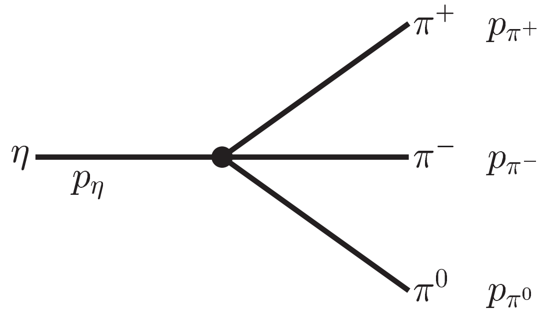

Figure 1: The kinematical variables in the decay $\eta \to \pi^+\pi^-\pi^0$.

Many applications exist, see e.g. the miniproceedings of the Bad Honnef meetings and the review articles[19] as well as the lectures [20].

3 $\eta \to \pi\pi\pi$ at order $\mathbf{p^4}$

3.1 Kinematics and Isospin Relations

The η is an isospin singlet and a pseudo-scalar. The decay into two pions is forbidden by CP. CP violation in η decays is discussed by C. Jarlskog and E. Shabalin[21] and J. Ng[22] in these proceedings. Three pions in an angular momentum 0 configuration cannot have isospin zero as well, but isospin 1 is allowed. This decay thus has to proceed via isospin breaking effects. Electromagnetism is known to play a fairly minor role here as discussed below, except via the kinematical effects due to the charged and neutral pion mass difference. This decay thus goes primarily through the strong isospin breaking part of QCD

$$\mathcal{L}_{\not{I}} = -\frac{1}{2}(m_u - m_d)\left(\bar{u}u - \bar{d}d\right) . \tag{11}$$

This itself has isospin 1 and there is thus to lowest order in isospin breaking a relation between $\eta \to \pi^+\pi^-\pi^0$ and $\eta \to \pi^0\pi^0\pi^0$.

The kinematics is depicted in Fig. 1.

The variables used in the remainder are

$$\begin{aligned} s &= \left(p_{\pi^+} + p_{\pi^-}\right)^2 = \left(p_\eta - p_{\pi^0}\right)^2 , \\ t &= \left(p_{\pi^-} + p_{\pi^0}\right)^2 = \left(p_\eta - p_{\pi^+}\right)^2 , \\ u &= \left(p_{\pi^+} + p_{\pi^0}\right)^2 = \left(p_\eta - p_{\pi^-}\right)^2 , \end{aligned} \tag{12}$$

which satisfy

$$s + t + u = m_\eta^2 + 2m_{\pi^+}^2 + m_{\pi^0}^2 \equiv 3s_0 . \tag{13}$$

The last equality is the definition of s_0.

The decay amplitude itself can be written as

$$\langle \pi^0\pi^+\pi^- \mathrm{out}|\eta\rangle = i\,(2\pi)^4\ \delta^4\left(p_\eta - p_{\pi^+} - p_{\pi^-} - p_{\pi^0}\right)\ A(s,t,u)\,. \tag{14}$$

Charge conjugation requires this amplitude to be symmetric under the interchange of π^+ and π^- so we have

$$A(s,t,u) = A(s,u,t)\,. \tag{15}$$

Using isospin as discussed above and labeling the three momenta as p_1, p_2, p_3 and $s_i = (p_\eta - p_i)^2$, the amplitude for the neutral decay

$$\langle \pi^0\pi^0\pi^0 \mathrm{out}|\eta\rangle = i\,(2\pi)^4\ \delta^4\left(p_\eta - p_1 - p_2 - p_3\right)\ \overline{A}(s_1,s_2,s_3) \tag{16}$$

satisfies

$$\overline{A}(s_1,s_2,s_3) = A(s_1,s_2,s_3) + A(s_2,s_3,s_1) + A(s_3,s_1,s_2)\,, \tag{17}$$

see e.g. [23] for a detailed derivation of this result. Experimentally, there are two main numbers to be kept in mind[24]. The decay width from an overall fit

$$\Gamma(\eta\to\pi^+\pi^-\pi^0) = 271 \pm 25\ eV\,, \tag{18}$$

with a scale factor of $S=1.8$, and the ratio of neutral to charged decays

$$r \equiv \frac{\Gamma(\eta\to\pi^0\pi^0\pi^0)}{\Gamma(\eta\to\pi^+\pi^-\pi^0)} = 1.404 \pm 0.034\,, \tag{19}$$

with a scale factor of $S=1.3$. The presence of these scale factors is an indication of mutually incompatible experiments.

3.2 Lowest order: p^2

The lowest order CHPT contribution from the quark mass difference was derived in the sixties using current algebra methods[25] and is

$$A(s,t,u) = \frac{B_0(m_u-m_d)}{3\sqrt{3}F_\pi^2}\left\{1 + \frac{3(s-s_0)}{m_\eta^2 - m_\pi^2}\right\}\,. \tag{20}$$

As announced, the decay amplitude is proportional to $m_u - m_d$. We can now rewrite the amplitude in terms of Q, a combination of quark masses which is experimentally more easily accessible,

$$Q^2 \equiv \frac{m_s^2 - \hat{m}^2}{m_d^2 - m_u^2}\,, \tag{21}$$

where m_i stands for the up, down or strange current quark mass, and

$$\hat{m} = \frac{1}{2}(m_u + m_d)\,. \tag{22}$$

The decay rate can then be written as

$$A(s,t,u) = \frac{1}{Q^2}\frac{m_K^2}{m_\pi^2}(m_\pi^2 - m_K^2)\,\frac{M(s,t,u)}{3\sqrt{3}F_\pi^2}\,, \tag{23}$$

with at lowest order

$$M(s,t,u) = \frac{3s - 4m_\pi^2}{m_\eta^2 - m_\pi^2}\,. \tag{24}$$

It can alternatively be rewritten in terms of

$$R = \frac{m_s - \hat{m}}{m_d - m_u} \tag{25}$$

as

$$A(s,t,u) = -\frac{1}{4\sqrt{3}F_\pi^2 R}\left(3s - 4m_\pi^2\right)\,. \tag{26}$$

So if we have a good theoretical description of $M(s,t,u)$, we get an accurate determination of Q, since

$$\Gamma\left(\eta \to 3\pi\right) \propto |A|^2 \propto Q^{-4}\,. \tag{27}$$

Due to the high power, the error on Q can be made much smaller than its determination from meson mass ratios,

$$Q^2 = \frac{m_K^2}{m_\pi^2}\frac{m_K^2 - m_\pi^2}{(m_{K^0}^2 - m_{K^+}^2)_{\mathrm{QCD}}}(1 + O(m_{quark}^2)), \tag{28}$$

because this relation has much larger electromagnetic corrections[26].

In order to show the accuracy which can be obtained, we can input two different values of Q or R. We first use the value

$$\begin{aligned} R &= 40.8 \pm 3.2 \qquad [27]\,, \\ \Gamma(\eta \to \pi^+\pi^-\pi^0) &\approx 66 \text{ eV}\,, \\ r &= 1.51\,. \end{aligned} \tag{29}$$

The second one is where we use instead the fit done at p^6 order for the quark masses from the meson masses and the estimate of the kaon electromagnetic mass difference including higher order effects [28],

$$\begin{aligned} Q &= 20.0 \pm 1.5 \quad \text{or} \quad R \approx 29\,, \\ \Gamma(\eta \to \pi^+\pi^-\pi^0) &\approx 140 \text{ eV}\,. \end{aligned} \tag{30}$$

It is clear that a good understanding of $M(s,t,u)$ can lead to a very accurate determination of Q and R.

3.3 Electromagnetic effects

The lowest order contribution does not contribute directly to the decay rate. It only comes in via the electromagnetic mass difference of pions. This is very relevant for the actual values of the kinematical variables s, t, u in terms of the measured momenta, but this can be included in a simple fashion. That this decay could not be explained by its electromagnetic contributions has been known for a long time already[29].

The calculation of the purely electromagnetic contribution to the decay has also been pushed to one-loop level[30] and the total effect remains small.

The decay with an extra photon in the final state has been estimated as well. This could have had potentially a large impact, since it can proceed without extra isospin breaking. Fortunately, both a simplified analysis using Low's theorem[31] and a full analysis at one loop in CHPT[32] lead to a rather small result of the order of 1% of the decay width of $\eta \to 3\pi$.

The correct incorporation of the electromagnetic corrections also tells us which value for the pion mass should be introduced in the expression for the amplitude. It is the same for both decays and is the neutral pion mass but we need to include the correct physical masses in the phase-space integrals. This follows from adding to $\mathcal{L}_2$ the effective electromagnetic term

$$\mathcal{L}_2 \longrightarrow \mathcal{L}_2 + C\langle QUQU^\dagger\rangle\,, \tag{31}$$

with

$$\langle QUQU^\dagger\rangle = -\frac{2e^2}{F^2}\left(\pi^+\pi^- + K^+K^-\right) + \frac{2e^2}{3F^2}\pi_3^2\pi^+\pi^- + \dots\,. \tag{32}$$

There is no direct contribution to $\eta \to 3\pi$. The first term leads to an equal mass shift for the charged pion and charged kaon in the chiral limit. This fact is known as Dashen's theorem[33]. The second term generates a contribution through mixing. This may appear to be negligibly small, because it is of order $e^2(m_d - m_u)$. However, this matters in the ratio r. Taking these corrections into account tells us that the pion mass appearing in Eq. (26) is the neutral pion mass.

3.4 Conclusions from the tree level

- The total rate is off by a factor of about 4, depending on the precise inputs used.

- The ratio r is near its experimental value. The reason for this is discussed below.

- Second order isospin breaking effects are important in the phase-space. Since the latter is small, small terms are important there - they significantly lower r.

- The effective Lagrangian method is a very efficient tool to perform these calculations.

3.5 One-loop contribution

The amplitude can be expanded as

$$A(s,t,u) = A_2(s,t,u) + A_4(s,t,u) + \dots \tag{33}$$

A_2 has been calculated in the previous subsections. To evaluate $A_4(s,t,u)$, one needs to evaluate one-loop diagrams with $\mathcal{L}_2$ and tree diagrams with $\mathcal{L}_4$. This was done in Ref. [34]. The decay rate can now be written in the form of Eq. (23). From the expression in Ref. [34], it can be seen that the only free parameter coming in is L_3. This parameter can be determined from $\pi\pi$-scattering[16] or more accurately from K_{e4} decays[28, 35].

What one numerically finds is a very large enhancement over the lowest order expression,

$$\frac{\int dLIPS|A_2 + A_4|^2}{\int dLIPS|A_2|^2} = 2.4\,, \tag{34}$$

where $LIPS$ stands for Lorentz invariant phase-space. This enhancement has as one major source the large S-wave final state rescattering as was expected, see Ref. [36] and references therein. In Sect. 4 we will come back to estimates of this contribution to higher orders. This contributions is about half of the total enhancement found in Ref. [34].

3.6 r and slope parameters

Can r be very different from 1.5? The lowest order amplitude has a zero for $s = (4/3)m_\pi^2$. Higher order corrections are not expected to remove the zero and also not to move it very much. We can thus expect that the amplitude will remain roughly of the form

$$A(s,t,u) \approx b\left(s - X m_\pi^2\right)\,, \tag{35}$$

with X about 4/3. Given this form we see from Fig. 2 that unless the zero moves very much, the ratio r will remain close to 1.5. The reason for this relation between X and the ratio r is the isospin relation between the amplitudes for the neutral and charged decays.

At $\mathcal{O}(p^4)$ the ratio r is changed from the tree level prediction. It is now lowered to 1.43, bringing it into nice agreement with the observed ratio. Again, the relation between X, or more generally the slope measurements in the Dalitz plot, and r follows from isospin. This is discussed in detail in Ref. [34].

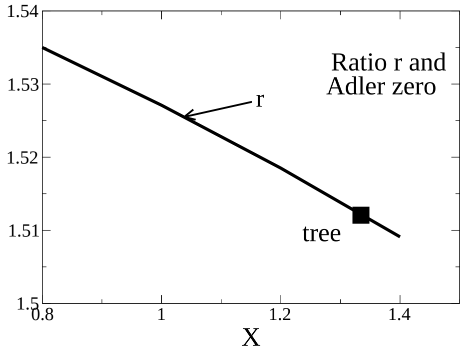

Figure 2: The dependence of r on X as defined in Eq. (35).

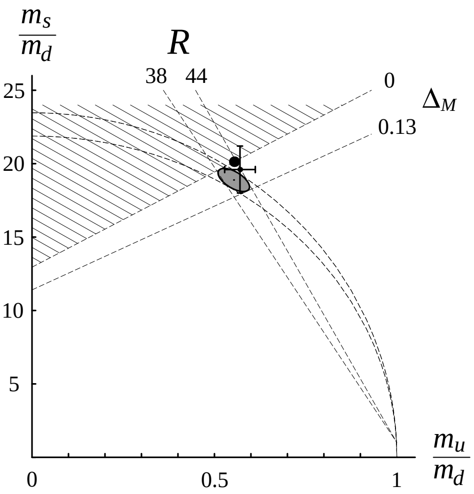

Figure 3: Leutwyler's ellipse and the constraints from mass differences at $\mathcal{O}(p^4)$. Taken from Ref. [27].

3.7 Q at order p^4

The quark mass ratio Q determines the major semi axis of Leutwyler's ellipse in the m_s/m_d and m_u/m_d plane[27],

$$\frac{m_u^2}{m_d^2} + \frac{1}{Q^2}\frac{m_s^2}{m_d^2} = 1\,. \tag{36}$$

The situation at order p^4 is shown in Fig. 3. The role that a better understanding of $\eta \to 3\pi$ has in this context is shown in Fig. 4, where at order p^4 the measurement of $\eta \to 3\pi$ is compared with the determination from the K^+-K^0 mass difference. The different points on the graph correspond to various estimates of the electromagnetic part of the mass difference. Note that estimates of

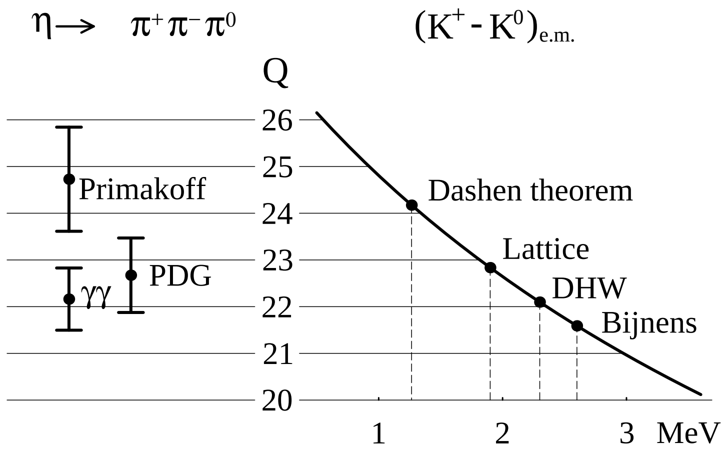

Figure 4: The importance of $\eta \to 3\pi$ for the measurement of Q. Taken from Ref. [27].

the p^6 contributions [28] indicate possibly even lower values of Q than are shown here.

4 $\eta \to \pi\pi\pi$ beyond order $\mathbf{p^4}$

4.1 The method and equations to solve

We can now try to estimate even higher orders using dispersion relation techniques. This should catch a large part of the higher order corrections, because the large $\pi\pi$ rescattering part was already a large part of the one-loop prediction. Unfortunately, for a general three-body decay, this is not such an easy undertaking. There are several subtleties involved here, as compared to the simple case of a two-body final state, because one can have imaginary parts not only from the scattering, but also from the unstable particle. The latter difficulty can be avoided by studying instead the scattering process $\pi\eta \to \pi\pi$ with an η mass such that the eta cannot decay. Then we only have $\pi\pi$ singularities in the various channels to deal with. This procedure is how one can restrict oneself to the influence of two-body scattering only. The general framework is known as Khuri-Treiman equations [37] and was used in Ref. [38] to study higher order corrections to eta decay.

Here we will restrict ourselves to a simpler formalism that has been very successful in the study of $\pi\pi$ scattering[39]. The underlying observation is that there are no imaginary parts from rescattering with angular momentum larger than or equal to two up to p^8. This together with the fact that $s + t + u$ is constant shows that to order p^6 the amplitude (23) can be written as

$$M(s,t,u) = M_0(s)+(s-u)M_1(t)+(s-t)M_1(t)+M_2(t)+M_2(u)-\frac{2}{3}M_2(s)\,. \quad (37)$$

The functions $M_I(s)$ correspond to isospin I rescattering in the two particles whose kinematics is described by s. The split into these functions is not quite unique. There is some ambiguity in the distribution of the polynomial terms over the various M_I, because $s+t+u$ is constant. The split (37) is useful because:

- Dispersion problems are now reduced to a set of functions of only *one* variable much simplifying the analysis.
- This split is fully correct to two-loop order.
- The main two-body rescattering corrections happen inside the functions M_I.

This method was used to estimate higher order corrections to $\eta \to 3\pi$ in Ref. [40]. A detailed description can be found in Ref. [23]. With the approximations used in Ref. [38], the two methods are in fact entirely equivalent.

So we use here the form (23) and discuss the process $\pi\eta \to \pi\pi$ with the final two pions in isospin I for an eta mass below the three pion threshold. This leads to the dispersion relations

$$M_I(s) = \frac{1}{\pi}\int_{4m_\pi^2}^{\infty} ds'\, \frac{\mathrm{Im}M_I(s')}{s'-s-i\varepsilon}\,, \quad (38)$$

up to subtractions, see below. To be more precise, the integrand contains the discontinuity

$$\mathrm{Im}M_I(s') \longrightarrow \mathrm{disc}M_I(s) = \frac{1}{2i}\left(M_I(s+i\varepsilon)-M_I(s-i\varepsilon)\right)\,. \quad (39)$$

We will need to subtract to be able to compare with the one-loop expression. Checking the high-energy behaviour of the one-loop expressions leads to three subtractions for M_0 and M_2, while two are sufficient for M_1. So the equations we will need to solve for M_I are

$$\begin{aligned}
M_0(s) &= a_0+b_0 s+c_0 s^2+\frac{s^3}{\pi}\int\frac{ds'}{s'^3}\,\frac{\mathrm{disc}M_0(s')}{s'-s-i\varepsilon}\,,\\
M_1(s) &= a_1+b_1 s+\frac{s^2}{\pi}\int\frac{ds'}{s'^2}\,\frac{\mathrm{disc}M_1(s')}{s'-s-i\varepsilon}\,,\\
M_2(s) &= a_2+b_2 s+c_2 s^2+\frac{s^3}{\pi}\int\frac{ds'}{s'^3}\,\frac{\mathrm{disc}M_2(s')}{s'-s-i\varepsilon}\,. \quad (40)
\end{aligned}$$

This leads to eight constants which should be determined. But the ambiguity in the precise choice of the M_I is visible here too. Up to the same order in the s,t,u expansion we have only four parameters

$$M(s,t,u) = a + bs + cs^2 - d(s^2+tu)\,, \tag{41}$$

so there is some freedom in the choice.

We can form some more convergent combinations at one-loop as well. Comparing expressions one sees that

$$M_0(s) + \frac{4}{3}M_2(s) \tag{42}$$

and

$$sM_1(s) + M_2(s) + s^2\frac{4L_3 - 1/(64\pi^2)}{F_\pi^2(m_\eta^2 - m_\pi^2)} \tag{43}$$

need only two subtractions. This allows to determine c and d in terms of L_3 and integrals over the discontinuities via

$$\begin{aligned} c &= c_0 + \frac{4}{3}c_2 = \frac{1}{\pi}\int \frac{ds'}{s'^3}\left\{\mathrm{disc}M_0(s') + \frac{4}{3}\mathrm{disc}M_2(s')\right\}\,, \\ d &= -\frac{4L_3 - 1/(64\pi^2)}{F_\pi^2(m_\eta^2 - m_\pi^2)} + \frac{1}{\pi}\int \frac{ds'}{s'^3}\left\{s'\mathrm{disc}M_1(s') + \mathrm{disc}M_2(s')\right\}\,. \end{aligned} \tag{44}$$

So once we know a, b and L_3, this forms a set of integral equations that can be solved. Now we have to put in the knowledge of the $\pi\pi$ phases. In a single channel problem without singularities in the cross channel, this problem is simple and was solved by Omnès long ago. Here we have cross-channel singularities but they are again $\pi\pi$ scattering in an isospin 0,1,2 state. The discontinuities thus obey[41]

$$\mathrm{disc}M_I(s) = \sin\delta_I(s)e^{-i\delta_I(s)}\left\{M_I(s) + \hat{M}_I(s)\right\}\,, \tag{45}$$

with $\hat{M}_I$ a consequence of the singularities in the t and u channel. They satisfy

$$\hat{M}_I(s) = \sum_{n,I'}\int_{-1}^{1} d\cos\theta\,\cos^n\theta\, c_{nII'}M_{I'}(t)\,, \tag{46}$$

where t is the appropriate t for a scattering of angle θ with center of mass energy squared of s. The coefficients $c_{nII'}$ can be found in [23, 41].

So at least we have a principle solution. There are several technical complications involved. After analytically continuing m_η^2 to its physical value, extra singularities appear, and we need $\hat{M}(s)$ for values of s outside the physical domain, so singularities in the relation of t with s and $\cos\theta$ appear. The integration path needs to be chosen carefully to avoid these extra singularities. Having solved this problem, one finds that the solution to the equations is not unique. The problem is that homogeneous equations of the type

$$M_I(s) = \frac{1}{\pi}\int \frac{ds'}{s'-s-i\varepsilon}\sin\delta_I(s)e^{-i\delta_I(s)}\left\{M_I(s)+\hat{M}_I(s)\right\} \tag{47}$$

have nontrivial solutions - we need to pick out the physically correct one. The solution is [40] to write a dispersion relation for a related function which only has one solution. We remove the singularity in the direct channel by dispersing instead

$$m_I(s) = \frac{M_I(s)}{\Omega_I(s)}\,, \tag{48}$$

with

$$\Omega_I(s) = \exp\left\{\frac{s}{\pi}\int\frac{ds'}{s'}\frac{\delta_I(s')}{s'-s-i\varepsilon}\right\}\,. \tag{49}$$

Similar arguments to above lead then to the dispersion relations with a total of 4 subtraction constants for the m_I. They are, rewritten in the M_I,

$$\begin{aligned}
\frac{M_0(s)}{\Omega_0(s)} &= \alpha_0+\beta_0 s+\gamma_0 s^2+\frac{s^2}{\pi}\int ds'\frac{\sin\delta_0(s')\,\hat{M}_0(s')}{|\Omega_0(s')|s'^2(s'-s-i\varepsilon)}\,,\\
\frac{M_1(s)}{\Omega_1(s)} &= \beta_1 s+\frac{s}{\pi}\int ds'\frac{\sin\delta_1(s')\,\hat{M}_1(s')}{|\Omega_1(s')|s'(s'-s-i\varepsilon)}\,,\\
\frac{M_2(s)}{\Omega_2(s)} &= \frac{s^2}{\pi}\int ds'\frac{\sin\delta_2(s')\,\hat{M}_2(s')}{|\Omega_2(s')|s'^2(s'-s-i\varepsilon)}\,.
\end{aligned} \tag{50}$$

So basically we now have to find a parametrization of $\delta_{0,1,2}(s)$, the $\pi\pi$ phase-shifts, and determine the subtraction constants. After that the above equations can be solved numerically. Two of the constants can be determined similarly to c and d above, leading to

$$\begin{aligned}
\gamma_0 &\approx 0\,,\\
\beta_1 &\approx -\frac{4L_3-1/(64\pi^2)}{F_\pi^2(m_\eta^2-m_\pi^2)}\,.
\end{aligned} \tag{51}$$

The values of these two parameters compared with the one-loop expressions are basically independent of the matching points. The other two are discussed in the next section.

4.2 Results

The two papers [40] and [38] basically only differ in the choice of the subtraction procedure. As explained above, the formalism is quite different but the underlying approximations and assumptions are the same.

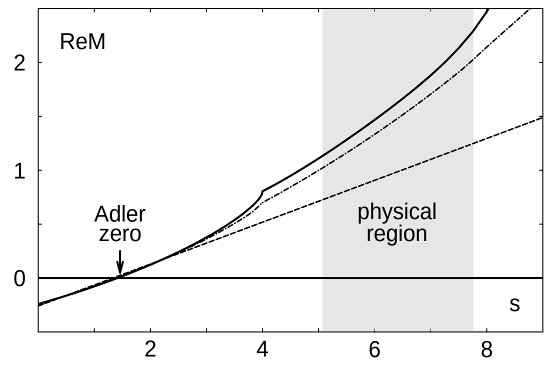

Figure 5: The result of Ref. [40] for Re$M(s,t,u)$ along the line $t = u$.

Reference [40] looks at the lowest order expression for

$$M(s,t,u) = \frac{3s - 4m_\pi^2}{m_\eta^2 - m_\pi^2}\,, \tag{52}$$

and notices that we can determine α_0 and β_0 from the place of the zero, the Adler zero happening at s_A, and the value of the slope in s at $s = s_A$.

Reference [38] instead uses several values of s, t, u to fit the dispersive approximation to the one-loop result. The resulting divergence in results is taken as an estimate of the theoretical error. The final result for the enhancement over the one-loop result is quite similar in both papers, but a closer look at the intermediate results shows some discrepancies which need to be understood. The one thing which can be compared are the published plots of Re$M(s,t,u)$ as a function of s along the line $t = u$. These are shown in Fig. 5 and 6. Notice that while both have a significant enhancement, the slope is quite different. The results of [40] are always above the one-loop result while the results of [38] cross the one-loop result at the end of the physical region. Given the similarity of the methods and the inputs used, this type of discrepancies needs to be understood, but it is obvious that a better experimental determination of the slopes can distinguish between both calculations. It is therefore very important that all slope parameters, see below for the definitions, are well measured.

As a simple estimate of the uncertainties involved, we have used a simplified version of the equations (50) where we set the functions $\hat{M}_I = 0$. So we only consider rescattering effects in the direct channel. We then fix the values of α_0 and β_0, considered real, to the tree level slope and Adler zero. In Fig. 7 the tree level is shown (tree) and the dispersive improved tree level (dispersive tree). The two dispersive improvements of the one-loop result shown are using the position of the one-loop Adler zero, and either the absolute value of the slope (dispersive

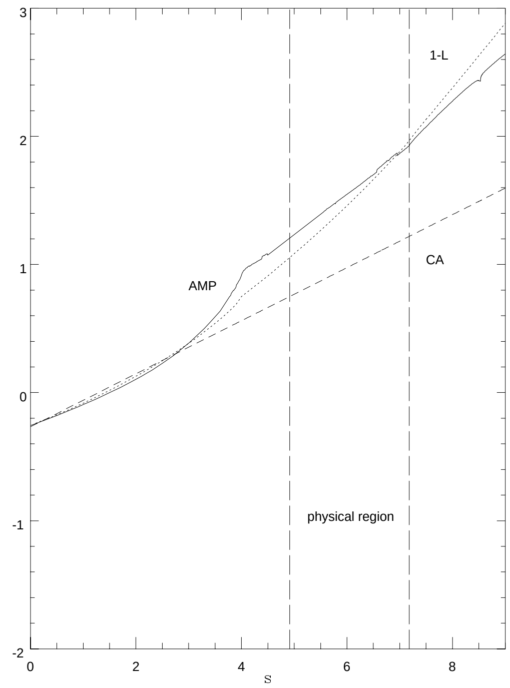

Figure 6: The result of Ref. [38] for Re$M(s,t,u)$ along the line $t=u$.

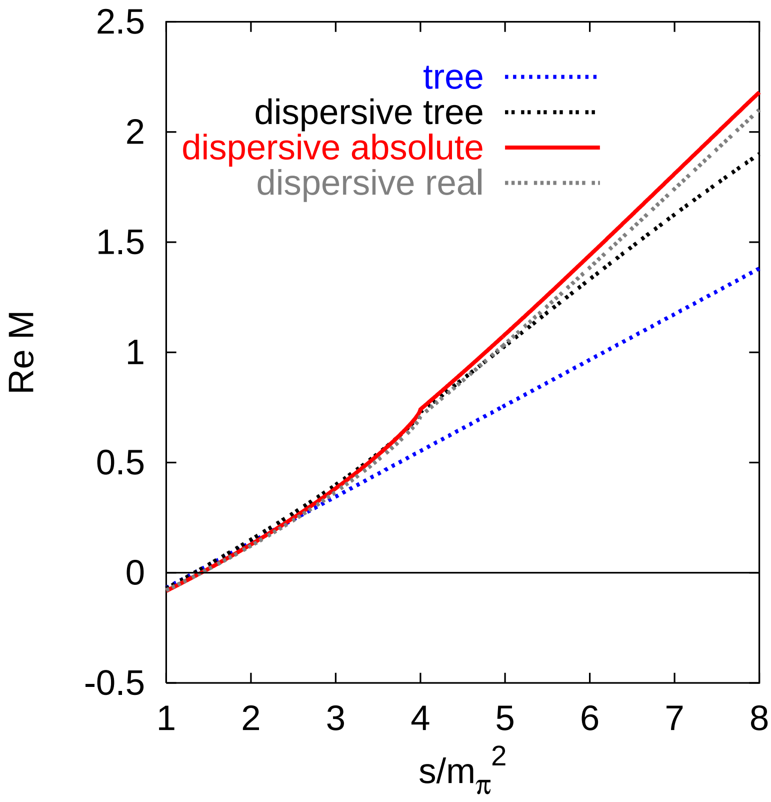

Figure 7: The value of Re$M(s,t,u)$ in a simplified version of the dispersion relations with several different estimates of the subtractions. α_0 and β_0 are determined from the tree level (dispersive tree) the position of the one-loop Adler zero, and either the absolute value of the slope (dispersive absolute) or its real part (dispersive real) at one-loop. The tree level (tree) result is shown for comparison.

absolute) or its real part (dispersive real) at one-loop to determine α_0 and β_0. It can be seen that these predictions lead to different slopes in the physical regions, thus allowing the theoretical subtraction procedure to be experimentally tested. Notice that we have shown only one variation in the phase-space. The variation over all of phase-space can of course be used similarly.

The total enhancement found is fairly small, about 14% in Ref. [38] for the total rate and 5% in the center of the Dalitz plot in Ref. [40], with a total rate enhancement in very good agreement with Ref. [38].

4.3 Dalitz plot expansions or slope parameters

Once the amplitude is known, one can easily expand the Dalitz plot distributions around the center of the Dalitz plot. Notice that some care is needed to precisely

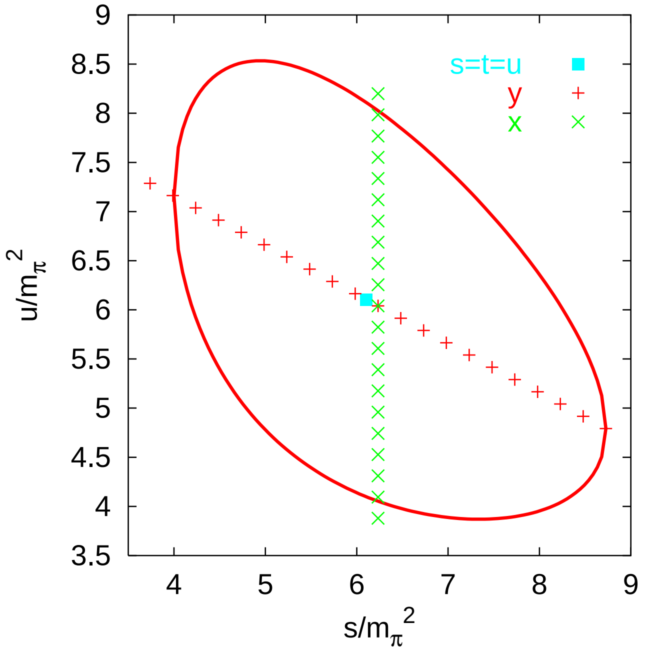

Figure 8: The Dalitz plot or phase-space of $\eta \to \pi^+\pi^-\pi^0$ decays. Shown are the boundaries of the physical region, the variation with x and y, see text, and the point $s = t = u$.

define the center of the Dalitz plot, given the second order isospin breakings discussed earlier. The point $s = t = u = s_0$ does not quite coincide with the point where all kinetic energies are equal for the charged decay. The usual definition of the slope parameters is in terms of the kinematical variables x and y,

$$\begin{aligned}
x &= \sqrt{3}\,\frac{T_+ - T_-}{Q_\eta} = \frac{\sqrt{3}}{2M_\eta Q_\eta}(u-t)\,,\\
y &= \frac{3T_0}{Q_\eta} - 1 = \frac{3}{2m_\eta Q_\eta}\left\{(m_\eta - m_{\pi^0})^2 - s\right\} - 1\,,\\
Q_\eta &= m_\eta - 2m_\pi^+ - m_\pi^0\,.
\end{aligned} \tag{53}$$

T_i stands for the kinetic energy of the pion of charge i. In Fig. 8 we have shown how s and u depend on x and y. The crosses correspond to $x = 0$ and y equal to -1, -0.9,…,1. The $\times$ correspond to $y = 0$ and $x = -1, 0.9, \ldots, 1$. The filled square indicates the place where $s = t = u$. The difference with the point $x = y = 0$ is again an indication of the isospin breaking effects in the masses discussed earlier.

The measured distribution is now parametrized as follows. For the charged decay, one takes

$$1 + ay + by^2 + cx^2\,, \tag{54}$$

	a	b	c	g
tree	-1.00	0.25	0.00	0.000
one-loop [34]	-1.33	0.42	0.08	0.03^a
dispersive [38]	-1.16	0.26	0.10	-0.014 — -0.028
tree dispersive	-1.10	0.31	0.001	-0.013
absolute dispersive	-1.21	0.33	0.04	-0.014

Table 1: Theoretical results for the slope parameters of the various approximations discussed in the text. The spread gives an indication of the uncertainty, for g it is about a factor two, even if the central values agree much better, see e.g. the discussion in [38]. [a]Ref. [34] does not quote a numerical value for g. We have obtained $g = 0.03$ from the representation of the amplitude provided in [34].

normalized to the center $x = y = 0$ of the Dalitz plot, and

$$1 + g(x^2 + y^2) \tag{55}$$

for the neutral decay. It is hard to compare with the experimental results in the review of particle properties [24]. They simply state that the assumptions made in the different measurements are not compatible. The problem is that making assumptions on the values of the quadratic slopes significantly alters the fitted result of the others. In table 1 we show the theoretical results of tree level, one-loop, the dispersive results from [38] and the results of the tree dispersive and absolute dispersive simplified estimates discussed above. Note that the one-loop predictions of the neutral slope g is not zero, contrary to the statement made in Refs. [42, 48]. The loops themselves do give a contribution, whereas the contributions from the tree and tadpole diagrams at $\mathcal{O}(p^4)$ happen to vanish. The precise value is dependent on the procedure used and is sensitive to fairly small changes. The number quoted corresponds to the precise way the expressions are given in [34]. We plan to come back to this issue in a later publication.

Measurements as mentioned earlier are difficult to compare, but several new results have been obtained recently. In particular, the new Crystal Ball value for g was announced at this meeting [49]. Note that the experiments usually quote $\alpha = g/2$. For completeness the known experimental results are given in table 2 for the charged decay and table 3 for the neutral decay.

Notice that while the overall agreement is all right, there is a problem in obtaining a value of g which is compatible with the newer experiments. The theoretical evaluation of g suffers from large cancellations.

	a	b	c
Layter[43]	-1.08 ± 0.14	0.034 ± 0.027	0.046 ± 0.031
Gormley[44]	-1.17 ± 0.02	0.21 ± 0.03	0.06 ± 0.04
Crystal Barrel[45]	-0.94 ± 0.15	0.11 ± 0.27	
Crystal Barrel[46]	-1.22 ± 0.07	0.22 ± 0.11	0.06 fixed

Table 2: Experimental results for the slope parameters in the charged decay.

	g
Alde[47]	-0.044 ± 0.046
Crystal Barrel[48]	-0.104 ± 0.039
Crystal Ball[49, 42]	-0.062 ± 0.008

Table 3: Experimental results for the slope parameter in the neutral decay. We have added in quadrature the statistical and systematical errors quoted in [48].

5 Dalitz and double Dalitz decays

This section is a shortened version of the work presented in Ref. [50]. The underlying question is how well do we understand the couplings of the η to two photons. In table 4 we show the (expected) branching ratios for all of the decays with two photons. The decays with one lepton-antilepton pair are known as Dalitz decays, those with two pairs as double Dalitz decays. These decays allow us to study the *off-shell* structure of the $\eta\gamma\gamma$ vertex as shown in Fig. 9. The question is: how does this form-factor $F(q_1^2, q_2^2)$ behave over the entire range of off-shell masses for the photons? Is it of order 1, w.r.t. to on-shell photons, can it be described by adding vector meson propagators in the photon legs? One would also like to

Decay	Branching ratio
$\eta \to \gamma\gamma$	39.33 ± 0.25 %
$\eta \to \gamma e^+e^-$	$(4.9 \pm 1.1) \cdot 10^{-3}$
$\eta \to \gamma\mu^+\mu^-$	$(3.1 \pm 0.4) \cdot 10^{-4}$
$\eta \to e^+e^-e^+e^-$	$\sim 6 \cdot 10^{-5}$
$\eta \to e^+e^-\mu^+\mu^-$	$\sim 2 \cdot 10^{-6}$
$\eta \to \mu^+\mu^-\mu^+\mu^-$	$\sim 10^{-8}$

Table 4: The measured or expected branching ratios for various decays of η to two (possibly off-shell) photons.

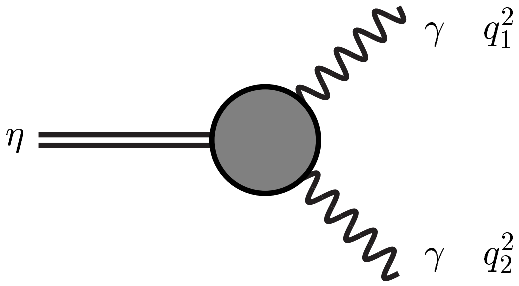

Figure 9: The $\eta\gamma\gamma$ vertex with photons of mass squared q_1^2 and q_2^2.

know the approach to the perturbative QCD result (see e.g. Ref. [51])

$$F(-Q^2,-Q^2) = \frac{8\pi^2 F_\pi^2}{3Q^2} + \dots\,, Q^2 \to \infty\,. \tag{56}$$

This type of form-factors are one of the places where experiments are possible for the same underlying physical process over the entire regime, ranging from the fully perturbative to the fully nonperturbative one. The large and intermediate values of $|q_1^2|$ and $|q_2^2|$ can be studied in tagged photon-photon collisions while the small timelike values can be studied in η-decays.

To study how well η-decays can see variations in the form-factor, in Ref. [50] four trial form-factors were investigated,

$$F(q_1^2,q_2^2) = 1\,, \tag{57}$$

$$= \frac{m_V^4}{(m_V^2-q_1^2)\,(m_V^2-q_2^2)}\,, \tag{58}$$

$$= \frac{m_V^2}{(m_V^2-q_1^2-q_2^2)}\,, \tag{59}$$

$$= \frac{m_V^4-(4\pi^2F_\pi^2/3)\,(q_1^2+q_2^2)}{(m_V^2-q_1^2)\,(m_V^2-q_2^2)}\,. \tag{60}$$

The first form is included to check how well a deviation from a pointlike eta can actually be measured. The second one is the standard double vector meson dominance model, while the third was a variation that reproduced single vector meson dominance, while numerically approaching Eq. (56) quite well. The last form was suggested in Ref. [52], see also Ref. [53], Knecht and Nyffeler in Ref. [54] as well as the contribution by Feldmann and Kroll to this conference[13]. One important reason why we like to know this form-factor better is that pseudoscalar exchange is the major contribution to the hadronic light-by-light scattering part of the muon anomalous magnetic moment as studied in Ref. [54]. The contribution of the exchange of π^0, η and η' using the different form-factors to $a_\mu = (g_\mu - 2)/2$

Decay	$m_{e^+e^-}\|_{\text{min}}$	(57)	(58),(59)	(60)
$\eta \to \gamma e^+ e^-$	$2m_e$	$1.62 \cdot 10^{-2}$	$1.67 \cdot 10^{-2}$	$1.66 \cdot 10^{-2}$
	50 MeV	$4.6 \cdot 10^{-3}$	$5.1 \cdot 10^{-3}$	$5.0 \cdot 10^{-3}$
	200 MeV	$8.6 \cdot 10^{-4}$	$11.5 \cdot 10^{-4}$	$10.9 \cdot 10^{-4}$
	300 MeV	$2.2 \cdot 10^{-4}$	$3.6 \cdot 10^{-4}$	$3.3 \cdot 10^{-4}$
	400 MeV	$3.0 \cdot 10^{-5}$	$6.3 \cdot 10^{-5}$	$5.6 \cdot 10^{-4}$
$\eta \to \gamma \mu^+ \mu^-$	—	$5.5 \cdot 10^{-4}$	$7.7 \cdot 10^{-4}$	$7.3 \cdot 10^{-4}$

Table 5: The branching ratios for the single Dalitz decays relative to $\eta \to \gamma\gamma$ as a function of the lower limit of the lepton pair mass for the different form-factors defined in the text.

Decay	$m_{e^+e^-}\|_{\text{min}}$	(58)	(59)	(60)
$\eta \to e^+ e^- \mu^+ \mu^-$	$2m_e$	$5.6 \cdot 10^{-6}$	$5.6 \cdot 10^{-6}$	$5.3 \cdot 10^{-6}$
	50 MeV	$11.6 \cdot 10^{-7}$	$11.7 \cdot 10^{-7}$	$10.9 \cdot 10^{-7}$
	200 MeV	$5.0 \cdot 10^{-8}$	$5.2 \cdot 10^{-8}$	$4.7 \cdot 10^{-8}$
	300 MeV	$2.8 \cdot 10^{-10}$	$2.9 \cdot 10^{-10}$	$2.6 \cdot 10^{-10}$

Table 6: The branching ratios for the double Dalitz decay $\eta \to e^+ e^- \mu^+ \mu^-$ relative to $\eta \to \gamma\gamma$ as a function of the lower limit of the electron positron pair mass for the different form-factors defined in the text.

is [50, 54] $7.9 \cdot 10^{-10}$ for form-factor (58), $9.7 \cdot 10^{-10}$ for (59) and $10.9 \cdot 10^{-10}$ for (60). It is thus clearly important for future measurements of a_μ that this form-factor becomes experimentally more constrained.

In tables 5 to 7 we show the results [50] for the various decays as a function of the electron-positron mass lower bound as well the muonic cases for all of phase-space. It turns out that it is surprisingly difficult to see the difference between the various models of the form-factors in η decays, but some constraints are possible. The form-factors which are different in single Dalitz decays should be easily distinguishable, but more subtle differences, as the one between (58) and (59) - which only become visible in double Dalitz decays - will be difficult to see. Given the importance of these results, the measurements should be performed. The differences between the effects of the the form-factors in (57) to (60) is $\mathcal{O}(p^6)$. Form-factors (58) (59) only differ at $\mathcal{O}(p^8)$. The differences are a good indication of the importance of the various orders.

6 $\eta \to \pi^0 \gamma\gamma$

This decay is only touched upon in this report. A more comprehensive discussion can be found in the review by Ametller[2] and in the references. The main theory

Decay	$m_{e^+e^-}\|_{\min}$	(58)	(59)	(60)
$\eta \to e^+e^-e^+e^-$	$2m_e$	$6.7 \cdot 10^{-5}$	$6.7 \cdot 10^{-5}$	$6.6 \cdot 10^{-5}$
	50 MeV	$4.4 \cdot 10^{-6}$	$4.4 \cdot 10^{-6}$	$4.3 \cdot 10^{-6}$
	100 MeV	$7.4 \cdot 10^{-7}$	$7.5 \cdot 10^{-7}$	$7.2 \cdot 10^{-7}$
	200 MeV	$2.7 \cdot 10^{-9}$	$2.8 \cdot 10^{-9}$	$2.6 \cdot 10^{-9}$
$\eta \to \mu^+\mu^-\mu^+\mu^-$	—	$9.2 \cdot 10^{-9}$	$9.4 \cdot 10^{-9}$	$8.5 \cdot 10^{-9}$

Table 7: The branching ratios for the double Dalitz decays $\eta \to \mu^+\mu^-\mu^+\mu^-$ and $\eta \to e^+e^-e^+e^-$ relative to $\eta \to \gamma\gamma$ as a function of the lower limit of the electron positron pair mass for the different form-factors defined in the text. The last line was not published earlier.

paper underlying this decay is [55], and the main interest is that this decay is a window on rather high order corrections in CHPT. The $\mathcal{O}(p^4)$ result is small for several reasons. The amplitude has two possible Lorentz structures. In the gauge $\epsilon_i \cdot q_j = 0$, with ϵ_i and q_i the polarization vector and momentum of photon i, the amplitude can be written as

$$M(\eta \to \pi^0\gamma\gamma) = A q_1 \cdot q_2\, \epsilon_1 \cdot \epsilon_2 - B\left(\epsilon_1 \cdot \epsilon_2\, P_\eta \cdot q_1\, P_\eta \cdot q_2 + P_\eta \cdot \epsilon_1\, P_\eta \cdot \epsilon_2\, q_1 \cdot q_2\right) . \tag{61}$$

At $\mathcal{O}(p^4)$ only the A part of the amplitude is nonzero and it is small. The pion loop is suppressed by isospin breaking and the kaon loop is suppressed by $4m_K^2$ and an extra factor of 1/12 in the integral. The contributions are

$$\begin{aligned} \pi\text{-loops} &\quad 0.84 \cdot 10^{-3}\ \text{eV}\,, \\ K\text{-loops} &\quad 2.45 \cdot 10^{-3}\ \text{eV}\,, \\ \text{sum} &\quad 3.9 \cdot 10^{-3}\ \text{eV}\,, \end{aligned} \tag{62}$$

rather far from the old experimental value of 0.84 ± 0.18 eV[24]. Newer experimental limits come from Novosibirsk[56] and the Crystal Ball[49]. The latter gives 0.42 ± 0.14 eV. The result of Eq. (62) is therefore more than two orders of magnitudes below the measured width.

We can also add vector meson exchange as depicted in Fig. 10. This starts at $\mathcal{O}(p^6)$ and has contributions to all orders. Restricting the exchange of ω and ρ to p^6 terms only leads to $\Gamma^{(6)}_{\rho,\omega} = 0.18$ eV and if all orders are kept

$$\Gamma_{\text{VMD}} = 0.31\ \text{eV}\,, \tag{63}$$

much larger than the suppressed p^4 contributions. In fact, there is one more contribution with well determined signs which appears at $\mathcal{O}(p^8)$. Here there is no isospin suppression of the pion-loops any longer nor any factors like the 1/12 at $\mathcal{O}(p^4)$. As a result the p^8 contribution from the double WZW vertex one-loop diagram is as large as the p^4 one. Given the structure of the amplitude,

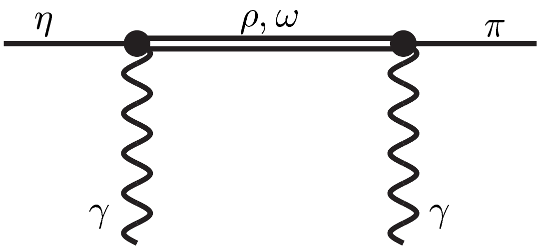

Figure 10: The vector meson exchange contribution to $\eta \to \pi^0\gamma\gamma$.

interference effects are quite strong so that if we put in the loops plus the VMD estimates we obtain the estimate[55]

$$\Gamma \approx 0.42 \text{ eV}. \tag{64}$$

We can now add the contribution from a_0 and a_2 exchange, the absolute values are experimentally known but the signs are free. This leads to

$$\Gamma \approx 0.42 \pm 0.20 \text{ eV}. \tag{65}$$

in very nice agreement with the preliminary Crystal Ball result. Studies of distributions in the decays will allow to disentangle various contributions to this decay. It should be noted that studies of this decay mode have also been performed in the ENJL model[57] and by adding other resonances than the ones referred to above[58]. There also exist some recent quark model studies[59].

7 Conclusions

We have discussed several eta decays from the point of view of Chiral Perturbation Theory and various possible enhancements. The main conclusion is that more and precise measurements are very much needed.

$\underline{\eta \to 3\pi}$: This decay has the potential to deliver accurate quark mass ratios. For this we need better measurements of the slope parameters in the Dalitz plot and a better determination of the ratio r between the neutral and charged decay mode. These will allow to put the theoretical calculations of the decay rate on the experimentally verified footing needed to obtain accurate quark mass ratios. A possible discrepancy with the slope g in the neutral decay should be checked theoretically and further experimental confirmation would be welcome.

$\underline{\eta \to \gamma^*\gamma^*}$: The double off-shell form-factors are needed in these double Dalitz decays and provide a useful insight into short-distance long-distance transitions in

QCD. They are also needed input in precision calculations for the muon anomalous magnetic moment. It turned out to be surprisingly difficult to see these differences in η-decays, but it is an important measurement to be performed.

$\underline{\eta \to \pi^0\gamma\gamma}$: The existing discrepancy with theory seems to be on the way to be resolved but we need confirmation of this and the study of distributions will allow different contributions to this decay mode to be distinguished. It is a decay mode where the usually dominant contributions CHPT at tree level and one-loop are very small. It thus provides a rare window on higher order contributions.

Acknowledgments

This work is supported by the Swedish Research Council, the Swiss National Science Foundation and the European Union TMR network, Contract No. ERB-FMRX–CT980169 (EURODAPHNE), and BBW-Contract No. 97.0131. We thank the local organizing committee for a well run and stimulating meeting and the sponsors, the Swedish Research Council, the Royal Swedish Academy of Sciences through its Nobel Institute for Physics and the Swedish Foundation for International Cooperation in Research and Higher Education. We thank Heiri Leutwyler for reading the manuscript.

References

[1] Holstein, B., these proceedings [hep-ph/0112150]

[2] Ametller, Ll., these proceedings [hep-ph/0111278]

[3] Luscher, M., Commun. Math. Phys. **105**, 153 (1986).

[4] Aoki, S. *et al.* [CP-PACS Collaboration], Nucl. Phys. Proc. Suppl. **106** (2002) 230 [arXiv:hep-lat/0110151];
Liu, C. a., Zhang, J. h., Chen, Y. and Ma, J. P., [hep-lat/0109020];
Liu, C. a., Zhang, J. h., Chen, Y. and Ma, J. P., [hep-lat/0109010].

[5] Weinberg, S., Physica A **96**, 327 (1979);
Leutwyler, H., Annals Phys. **235**, 165 (1994) [hep-ph/9311274].

[6] Colangelo, G., Gasser, J. and Leutwyler, H., Phys. Lett. B **488**, 261(2000) [hep-ph/0007112].

[7] Weinberg, S., Phys. Rev. Lett. **17**, 616 (1966).

[8] Gasser, J. and Leutwyler, H., Phys. Lett. B **125**, 325 (1983).

[9] Bijnens, J., Colangelo, G., Ecker, G., Gasser, J. and Sainio, M. E., Phys. Lett. B **374**, 210 (1996) [hep-ph/9511397]; Nucl. Phys. B **508**, 263 (1997) [Erratum-ibid. B **517**, 639 (1997)] [hep-ph/9707291].

[10] Bass, S. D., these proceedings, [hep-ph/0111180].

[11] Shore, G., these proceedings [hep-ph/0111165].

[12] Michael, C., these proceedings [hep-lat/0111056].

[13] Feldmann, T. and Kroll, P., these proceedings, [hep-ph/0201044].

[14] Gell-Mann, M., Oakes, R. J. and Renner, B., Phys. Rev. **175**, 2195 (1968).

[15] Weinberg, S., Phys. Rev. **166**, 1568 (1968).

[16] Gasser, G. and Leutwyler, H., Nucl. Phys. B **250**, 465 (1985).

[17] Bijnens, J., Colangelo, G. and Ecker, G., Annals Phys. **280** 100 (2000). [hep-ph/9907333].

[18] Heitger, J., Sommer, R. and Wittig, H. [ALPHA Collaboration], Nucl. Phys. B **588** 377 (2000) [hep-lat/0006026];
Irving, A. C., McNeile, C., Michael, C., Sharkey, K. J. and Wittig, H. [UKQCD Collaboration], Phys. Lett. B **518**, 243 (2001) [hep-lat/0107023].

[19] Bijnens, J. and Meißner, U.-G., Workshop on the Standard Model at low Energies, ECT*, Trento, 1996, Miniproceedings [hep-ph/9606301];
Bijnens, J. and Meißner, U.-G., Workshop on Chiral Effective Theories, Bad Honnef, 1998, Miniproceedings [hep-ph/9901381];
Bijnens, J., Meissner, U.-G. and Wirzba, A., Workshop on Effective Field Theories of QCD, Bad Honnef, 2001, [hep-ph/0201266];
Ecker, G., Prog. Part. Nucl. Phys. **35**, 1 (1995) [hep-ph/9501357];
Bernard, V., Kaiser, N. and Meissner, U.-G., Int. J. Mod. Phys. E **4**, 193 (1995) [hep-ph/9501384].

[20] Pich, A., Lectures at Les Houches Summer School in Theoretical Physics, Session 68: Probing the Standard Model of Particle Interactions, Les Houches, France, 28 Jul - 5 Sep 1997, [hep-ph/9806303];
Ecker, G., Lectures given at Advanced School on Quantum Chromodynamics (QCD 2000), Benasque, Huesca, Spain, 3-6 Jul 2000, [hep-ph/0011026].

[21] Jarlskog, C. and Shabalin, E., these proceedings.

[22] Ng, J. N., these proceedings.

[23] Walker, M., "$\eta \to 3\pi$", Master Thesis, Bern University (1998). Can be obtained from `http://www-itp.unibe.ch/research.shtml#diploma`.

[24] Groom, D. E. *et al.* [Particle Data Group Collaboration], Eur. Phys. J. C **15**, 1 (2000).

[25] Bell, J. S. and Sutherland, D. G., Nucl. Phys. B **4**, 315 (1968);
Cronin, J. A., Phys. Rev. **161**, 1483 (1967).

[26] Donoghue, J. F., Holstein, B. R. and Wyler, D., Phys. Rev. D **47**, 2089 (1993);
Bijnens, J., Phys. Lett. B **306**, 343 (1993) [hep-ph/9302217];
Bijnens, J. and Prades, J., Nucl. Phys. B **490**, 239 (1997) [hep-ph/9610360].

[27] H. Leutwyler, H., Phys. Lett. B **378**, 313 (1996) [hep-ph/9602366].

[28] Amoros, G., Bijnens, J. and P. Talavera, P., Nucl. Phys. B **602**, 87 (2001) [hep-ph/0101127].

[29] Sutherland, D. G., Nucl. Phys. B **2**, 433(1967);
Dittner, P., Eliezer, S. and Dondi, P. H., Phys. Rev. D **8**, 2253 (1973).

[30] Baur, R., Kambor, J. and Wyler, D., Nucl. Phys. B **460**, 127 (1996). [hep-ph/9510396].

[31] Bramon, A., Gosdzinsky, P. and Tortosa, S., Phys. Lett. B **377**, 140 (1996) [hep-ph/9603357].

[32] D'Ambrosio, G., Ecker, G., Isidori, G. and Neufeld, H., Phys. Lett. B **466**, 337 (1999) [hep-ph/9905420].

[33] Dashen, R. F., Phys. Rev. **183**, 1245 (1969).

[34] Gasser, J. and Leutwyler, H., Nucl. Phys. B **250**, 539 (1985).

[35] Amoros, G., Bijnens, J. and Talavera, P., Phys. Lett. B **480**, 71 (2000) [hep-ph/9912398];
Nucl. Phys. B **585**, 293 (2000) [Erratum-ibid. B **598**, 665 (2000)] [hep-ph/0003258].

[36] Roiesnel, C. and Truong, T., Nucl. Phys. B **187**, 293 (1981).

[37] Khuri, N. N. and Treiman, S. B., Phys. Rev. **119**, 1115 (1960);
Kacser, C., Phys. Rev. **132**, 2712-2721 (1963)

[38] Kambor, J., Wiesendanger, C. and Wyler, D., Nucl. Phys. B **465**, 215 (1996) [hep-ph/9509374].

[39] Knecht, M., Moussallam, B., Stern, J. and Fuchs, N. H., Nucl. Phys. B **471**, 445 (1996) [hep-ph/9512404].

[40] Anisovich, A. V. and Leutwyler, H., Phys. Lett. B **375**, 335 (1996) [hep-ph/9601237].

[41] Anisovich, A. V., Phys. Atom. Nucl. **58**, 1383 (1995) [Yad. Fiz. **58N8**, 1467 (1995)].

[42] Tippens, W. B. *et al.* [Crystal Ball Collaboration], Phys. Rev. Lett. **87**, 192001 (2001). Eq. (1c) in this paper contains a misprint: The $\sqrt{3}$ in the definition of y should be replaced by 3.

[43] Layter, J. G. *et al.*, Phys. Rev. D **7** (1973) 2565.

[44] Gormley, M. *et al.*, Phys. Rev. D **2**, 501 (1970).

[45] Amsler, C. *et al.* [Crystal Barrel Collaboration], Phys. Lett. B **346**, 203 (1995).

[46] Abele, A. *et al.* [Crystal Barrel Collaboration], Phys. Lett. B **417**, 197 (1998).

[47] Alde, D. *et al.* [Serpukhov-Brussels-Annecy(LAPP) Collaboration], Z. Phys. C **25**, 225 (1984) [Yad. Fiz. **40**, 1447 (1984)].

[48] Abele, A. *et al.* [Crystal Barrel Collaboration], Phys. Lett. B **417**, 193 (1998).

[49] Nefkens, B. and Price, J., these proceedings.

[50] Bijnens, J. and Persson, F., "Effects of different form-factors in meson photon photon transitions and the muon anomalous magnetic moment," [hep-ph/0106130]. (Master's thesis of F. Persson.)

[51] Novikov, V.A., M. A. Shifman, M. A., Vainshtein, A. I., Voloshin, M. B. and Zakharov, V. I., Nucl. Phys. B **237**, 525 (1984);
Nesterenko, V. A. and A. V. Radyushkin, A. V., Sov. J. Nucl. Phys. **38**, 284 (1983) [Yad. Fiz. **38**, 476 (1983)].

[52] Knecht, M., Peris, S., Perrottet, M. and de Rafael, E., Phys. Rev. Lett. **83**, 5230 (1999) [hep-ph/9908283].

[53] Knecht, M. and Nyffeler, A., Eur. Phys. J. C **21**, 659 (2001) [hep-ph/0106034].

[54] Knecht, M. and Nyffeler, A., [hep-ph/0111058];
Knecht, M., Nyffeler, A., Perrottet, M. and de Rafael, E., [hep-ph/0111059];
Hayakawa, M. and Kinoshita, T., Phys. Rev. D **57**, 465 (1998) [hep-ph/9708227];
Bijnens, J., Pallante, E. and Prades, J., Phys. Rev. Lett. **75**, 1447 (1995) [Erratum-ibid. **75**, 3781 (1995)] [hep-ph/9505251];

Bijnens, J., Pallante, E. and Prades, J., Nucl. Phys. B **474**, 379 (1996) [hep-ph/9511388];
Bijnens, J., Pallante, E. and J. Prades, J., [hep-ph/0112255];
Hayakawa, M. and Kinoshita, T., [hep-ph/0112102].

[55] Ametller, Ll., Bijnens, J., Bramon, A. and Cornet, F., Phys. Lett. B **276**, 185 (1992).

[56] Achasov, M. N. *et al.*, Nucl. Phys. B **600**, 3 (2001) [hep-ex/0101043].

[57] Nemoto, Y., Oka, M. and Takizawa, M., Phys. Rev. D **54**, 6777 (1996) [hep-ph/9602253];
Bijnens, J., Fayyazuddin, A. and Prades, J., Phys. Lett. B **379**, 209 (1996) [hep-ph/9512374];
Bel'kov, A. A., Lanyov, A. V. and Scherer, S., J. Phys. G **22**, 1383 (1996) [hep-ph/9506406];
Bellucci, S. and Bruno, C,, Nucl. Phys. B **452**, 626 (1995) [arXiv:hep-ph/9502243].

[58] Ko, P., Phys. Lett. B **349**, 555 (1995) [hep-ph/9503253];
Phys. Rev. D **47**, 3933 (1993).

[59] Ng, J. N. and Peters, D. J., Phys. Rev. D **47**, 4939 (1993).